

Evidence for a bottom baryon resonance  $\Lambda_b^{*0}$  in CDF dataPRABHAKAR PALNI (CDF COLLABORATION)<sup>1</sup>

*Department of Physics and Astronomy  
University of New Mexico, MSC07 4220, 1919 Lomas Blvd. NE,  
Albuquerque, NM 87131-0001, USA*

Using data from proton-antiproton collisions at  $\sqrt{s} = 1.96$  TeV recorded by the CDF II detector at the Fermilab Tevatron, evidence for the excited resonance state  $\Lambda_b^{*0}$  is presented in its  $\Lambda_b^0 \pi^- \pi^+$  decay, followed by the  $\Lambda_b^0 \rightarrow \Lambda_c^+ \pi^-$  and  $\Lambda_c^+ \rightarrow p K^- \pi^+$  decays. The analysis is based on a data sample corresponding to an integrated luminosity of  $9.6 \text{ fb}^{-1}$  collected by an online event selection based on charged-particle tracks displaced from the proton-antiproton interaction point. The significance of the observed signal is  $3.5\sigma$ . The mass of the observed state is found to be  $5919.22 \pm 0.76 \text{ MeV}/c^2$  in agreement with similar findings in proton-proton collision experiments.

PRESENTED AT

DPF 2013

The Meeting of the American Physical Society  
Division of Particles and Fields  
Santa Cruz, California, August 13–17, 2013

---

<sup>1</sup>Work supported by the U.S. Department of Energy.

# 1 Introduction

Baryons with a heavy quark  $Q$  are useful for probing quantum chromodynamics (QCD) in its confinement domain. Observing new heavy-quark baryon states and measuring their properties provides further experimental constraints to the phenomenology in this regime. This report provides an additional contribution to the currently small number of heavy quark baryon observations.

In the framework of heavy-quark effective theories (HQET) [1, 2], a bottom quark  $b$  and a spin-zero  $[ud]$  diquark, carrying an angular momentum  $L = 1$  relative to the  $b$  quark (hence named  $P$ -wave states), can form two excited states. These are named  $\Lambda_b^{*0}$ , with same quark content as the singlet  $\Lambda_b^0$  [3] and isospin  $I = 0$ , but total spin and parity  $J^P = \frac{1}{2}^-$  and  $J^P = \frac{3}{2}^-$  [4]. These isoscalar states are the lightest  $P$ -wave states that can decay to the  $\Lambda_b^0$  baryon via strong interaction processes. The decays require the emission of a pair of low-momentum (*soft*) pions. Both  $\Lambda_b^{*0}$  [5] particles are classified as bottom-baryon resonant states. Several recent theoretical predictions of their masses are available. An approach based on a quark-potential model with the color hyperfine interaction is used in Ref. [6]. The authors in Ref. [7] use a constituent quark model incorporating the basic properties of QCD and solving exactly the three-body problem. A heavy baryon is considered in Ref. [8] as a heavy-quark and light-diquark system in the framework of the relativistic quark model based on the quasipotential approach in QCD. The spectroscopy of isoscalar heavy baryons and their excitations is studied in Ref. [9] within the framework of HQET at leading and next-to-leading orders in the combined inverse heavy-quark mass,  $1/m_Q$ , and inverse number of colors,  $1/N_c$ , expansions. The nonperturbative formalism of QCD sum rules is applied within HQET to calculate the mass spectra of the bottom baryon states [10]. Some calculations predict  $\Lambda_b^{*0}$  masses smaller than the hadronic decay kinematic-threshold ( $\approx 5900 \text{ MeV}/c^2$ ), allowing only radiative decays [7, 10]. Other calculations predict the mass difference  $M(\Lambda_b^{*0}) - M(\Lambda_b^0)$  for the  $J^P = \frac{1}{2}^-$  state to be approximately in the range 300–310  $\text{MeV}/c^2$  [6, 8, 9]. The mass splitting between the two states is predicted to be in the range 10–17  $\text{MeV}/c^2$ .

The first experimental studies of  $b$ -quark baryon resonant states were reported by CDF with the observation of the  $S$ -wave states  $\Sigma_b^{(*)}$  in their  $\Lambda_b^0 \pi^\pm$  decays [11, 12]. The ground states of the charged bottom-strange  $\Xi_b^-$  baryon [13, 14, 15] and bottom doubly-strange  $\Omega_b^-$  [16, 15] were reported by both CDF and D0, and later CDF observed the neutral bottom-strange baryon  $\Xi_b^0$  [17]. Recently, LHCb reported precise mass measurements of the ground state  $\Lambda_b^0$ , the  $\Xi_b^-$  state, and the  $\Omega_b^-$  state [18]. The CMS collaboration observed another bottom-strange state,  $\Xi_b^{*0}$ , which is interpreted as a  $J^P = \frac{3}{2}^+$  resonance [19]. Most recently, two states, interpreted as the two  $\Lambda_b^{*0}$  resonant states were observed by the LHCb collaboration for the first time [20].

In this report, we present evidence for the production of a  $\Lambda_b^{*0}$  resonance state in CDF data. We search for candidate  $\Lambda_b^{*0}$  baryons produced in proton-antiproton

collisions at  $\sqrt{s} = 1.96$  TeV using a data sample from an integrated luminosity of  $9.6 \text{ fb}^{-1}$  collected by CDF with a specialized online event-selection (trigger) that collects events enriched in fully hadronic decays of  $b$  hadrons. The  $\Lambda_b^{*0}$  candidates are identified in the pseudorapidity range  $|\eta| < 1.0$  using their exclusive decays to  $\Lambda_b^0$  baryons and two oppositely-charged soft pions. The excellent performance of the CDF devices for measuring charged particle trajectories (tracks) allows reconstructing charged particles with transverse momenta as low as  $200 \text{ MeV}/c$ . The result in this paper is the first to support the LHCb observation [20].

## 2 The CDF II Detector

The component of the CDF II detector [21] most relevant to this analysis is the charged-particle tracking system, which operates in a uniform axial magnetic field of  $1.4 \text{ T}$  generated by a superconducting solenoidal magnet. The inner tracking system is comprised of a silicon tracker [22]. A large open-cell cylindrical drift chamber [23] completes the tracking system. The silicon tracking system measures the transverse impact parameter of tracks with respect to the primary interaction point,  $d_0$  [24], with a resolution of  $\sigma_{d_0} \approx 40 \mu\text{m}$ , including an approximately  $32 \mu\text{m}$  contribution from the beam size [22]. The transverse momentum resolution of the tracking system is  $\sigma(p_T)/p_T^2 \approx 0.07\%$  with  $p_T$  in  $\text{GeV}/c$  [24].

## 3 Data Sample and Simulation

This analysis relies on a three-level trigger to collect data samples enriched in multi-body hadronic decays of  $b$  hadrons (displaced-track trigger). The trigger requires two charged particles in the drift chamber, each with  $p_T > 2.0 \text{ GeV}/c$  [25]. The particle tracks are required to be azimuthally separated by  $2^\circ < \Delta\phi < 90^\circ$  [24]. Silicon information is added and the impact parameter  $d_0$  of each track is required to lie in the range  $0.12\text{--}1 \text{ mm}$  providing efficient discrimination of long-lived  $b$  hadrons [26]. Finally, the distance  $L_{xy}$  in the transverse plane between the collision space-point (primary vertex) and the intersection point of the two tracks projected onto their total transverse momentum is required to exceed  $200 \mu\text{m}$ .

The mass resolution of the  $\Lambda_b^{*0}$  resonances is predicted with a Monte-Carlo simulation that generates  $b$  quarks according to a calculation expanded at next-to-leading order in the strong coupling constant [27] and produces events containing final-state hadrons by simulating  $b$ -quark fragmentation [28]. In the simulations, the  $\Lambda_b^{*0}$  baryon is assigned the mass value of  $5920.0 \text{ MeV}/c^2$ . Decays are simulated with the EVTGEN [29] program, and all  $b$  hadrons are simulated unpolarized. The generated events are passed to a GEANT3-based [30] detector simulation, then to a trigger simulation, and finally the same reconstruction algorithm as used for experimental data.

The  $\Lambda_b^{*0}$  candidates are reconstructed in the exclusive strong-interaction decay  $\Lambda_b^{*0} \rightarrow \Lambda_b^0 \pi_s^- \pi_s^+$ , where the low-momentum pions  $\pi_s^\pm$  are produced near kinematic threshold [31]. The  $\Lambda_b^0$  baryon decays through the weak interaction to a baryon  $\Lambda_c^+$  and a pion, labeled as  $\pi_b^-$  to distinguish it from the soft pions. This is followed by the weak-interaction decay  $\Lambda_c^+ \rightarrow p K^- \pi^+$ . We search for a  $\Lambda_b^{*0}$  signal in the  $Q$ -value distribution, where  $Q = m(\Lambda_b^0 \pi_s^- \pi_s^+) - m(\Lambda_b^0) - 2 m_\pi$ ,  $m(\Lambda_b^0)$  is the reconstructed  $\Lambda_c^+ \pi_b^-$  mass, and  $m_\pi$  is the known charged-pion mass. The effect of the  $\Lambda_b^0$  mass resolution is suppressed, and most of the systematic uncertainties are reduced in the mass difference. We search for narrow structures in 6–45 MeV/ $c^2$  range of the  $Q$ -value spectrum motivated by the theoretical estimates [6, 8, 9] and the LHCb findings [20].

## 4 Analysis Overview

The analysis begins with the reconstruction of the  $\Lambda_c^+ \rightarrow p K^- \pi^+$  decay space-point by fitting three tracks to a common point. Standard CDF quality requirements are applied to each track, and only tracks corresponding to particles with  $p_T > 400$  MeV/ $c$  are used. No particle identification is used. All tracks are refitted using pion, kaon, and proton mass hypotheses to correct for the mass-dependent effects of multiple scattering and ionization-energy loss. The invariant mass of the  $\Lambda_c^+$  candidate is required to match the known value [3] within  $\pm 18$  MeV/ $c^2$ . The momentum vector of the  $\Lambda_c^+$  candidate is then extrapolated to intersect with a fourth track that is assumed to be a pion, to form the  $\Lambda_b^0 \rightarrow \Lambda_c^+ \pi_b^-$  candidate. The  $\Lambda_b^0$  reconstructed decay point (decay vertex) is subjected to a three-dimensional kinematic fit with the  $\Lambda_c^+$  candidate mass constrained to its known value [3]. The probability of the  $\Lambda_b^0$  vertex fit must exceed 0.01% [12]. The proton from the  $\Lambda_c^+$  candidate is required to have  $p_T > 2.0$  GeV/ $c$  to ensure that the proton is consistent with having contributed to the trigger decision. The minimum requirement on  $p_T(\pi_b^-)$  is determined by an optimization procedure, maximizing the quantity  $S_{\Lambda_b^0}/(1 + \sqrt{B})$  [32], where  $S_{\Lambda_b^0}$  is the number of  $\Lambda_b^0$  signal events obtained from the fit of the observed  $\Lambda_c^+ \pi_b^-$  mass distribution and  $B$  is the number of events in the sideband region of  $50 < Q < 90$  MeV/ $c^2$  scaled to the background yield expected in the signal range  $14.0 < Q < 26.0$  MeV/ $c^2$ . The sideband region boundaries are motivated by the signal predictions in Refs. [6, 8, 9]. The resulting requirement is found to be  $p_T(\pi_b^-) > 1.0$  GeV/ $c$ . The momentum criteria both for proton and  $\pi_b^-$  candidates favor these particles to be the two that contribute to the displaced-track trigger decision. To keep the soft pions from  $\Lambda_b^{*0}$  decays within the kinematic acceptance, the  $\Lambda_b^0$  candidate must have  $p_T(\Lambda_b^0) > 9.0$  GeV/ $c$ . This maximizes the quantity  $S_{MC}/(1 + \sqrt{B})$ , where  $S_{MC}$  is the  $\Lambda_b^{*0}$  signal reconstructed in the simulation.

To suppress prompt backgrounds from primary interactions, the decay vertex of the long-lived  $\Lambda_b^0$  candidate is required to be distinct from the primary vertex by

requiring the proper decay time and its significance to be  $ct(\Lambda_b^0) > 200 \mu\text{m}$  and  $ct(\Lambda_b^0)/\sigma_{ct} > 6.0$ , respectively. The first criterion validates the trigger condition, while the second is fully efficient on simulated  $\Lambda_b^{*0}$  signal decays. We define the proper decay time as  $ct(\Lambda_b^0) = L_{xy} m_{\Lambda_b^0} c/p_T$ , where  $m_{\Lambda_b^0}$  is the known mass of the  $\Lambda_b^0$  baryon [3]. We require the  $\Lambda_c^+$  vertex to be associated with a  $\Lambda_b^0$  decay by requiring  $ct(\Lambda_c^+) > -100 \mu\text{m}$ , as derived from the quantity  $L_{xy}(\Lambda_c^+)$  measured with respect to the  $\Lambda_b^0$  vertex. This requirement reduces contributions from  $\Lambda_c^+$  baryons directly produced in  $p\bar{p}$  interactions and from random combinations of tracks that accidentally are reconstructed as  $\Lambda_c^+$  candidates. To reduce combinatorial background and contributions from partially-reconstructed decays,  $\Lambda_b^0$  candidates are required to point towards the primary vertex by requiring the impact parameter  $d_0(\Lambda_b^0)$  not to exceed  $80 \mu\text{m}$ . The  $ct(\Lambda_c^+)$  and  $d_0(\Lambda_b^0)$  criteria [12] are fully efficient for the  $\Lambda_b^{*0}$  signal.

Figure 1 shows the resulting prominent  $\Lambda_b^0$  signal in the  $\Lambda_c^+\pi_b^-$  invariant mass distribution. The binned maximum-likelihood fit finds a signal of approximately 15 400 candidates at the expected  $\Lambda_b^0$  mass, with unity signal-to-background ratio. The fit model describing the invariant mass distribution comprises the Gaussian  $\Lambda_b^0 \rightarrow \Lambda_c^+\pi_b^-$  signal overlapping a background shaped by several contributions. Random four-track combinations dominating the right sideband are modeled with an exponentially decreasing function. Coherent sources populate the left sideband and leak under the signal. These include reconstructed  $B$  mesons that pass the  $\Lambda_b^0 \rightarrow \Lambda_c^+\pi_b^-$  selection criteria, partially reconstructed  $\Lambda_b^0$  decays, and fully reconstructed  $\Lambda_b^0$  decays other than  $\Lambda_c^+\pi_b^-$  (e.g.,  $\Lambda_b^0 \rightarrow \Lambda_c^+K^-$ ). Shapes representing the physical background sources are derived from Monte-Carlo simulations. Their normalizations are constrained to branching ratios that are either measured (for  $B$  meson decays, reconstructed within the same  $\Lambda_c^+\pi_b^-$  sample) or theoretically predicted (for  $\Lambda_b^0$  decays). The discrepancy between the fit and the data at smaller masses than the  $\Lambda_b^0$  signal is attributed to incomplete knowledge of the branching fractions of decays populating this region [33, 11, 34, 12] and is verified to have no effect on the final results. The fit is used only to define the  $\Lambda_b^{*0}$  search sample.

## 5 Experimental Mass Distribution and The Fit

To reconstruct the  $\Lambda_b^{*0}$  candidates, each  $\Lambda_b^0$  candidate with mass within the range  $5.561\text{--}5.677 \text{ GeV}/c^2$  ( $\pm 3\sigma$ ) is combined with a pair of oppositely-charged particles, each assigned the pion mass. To increase the efficiency for reconstructing  $\Lambda_b^{*0}$  decays near the kinematic threshold, the quality criteria applied to soft-pion tracks are loosened. The basic requirements for hits in the drift chamber and main silicon tracker are imposed on the  $\pi_s^\pm$  tracks, and tracks reconstructed with a valid fit, proper error matrix, and with  $p_T > 200 \text{ MeV}/c$  are accepted. The relaxed requirements on the soft-pion tracks increase the reconstructed  $\Lambda_b^{*0}$  candidates yield by a factor of

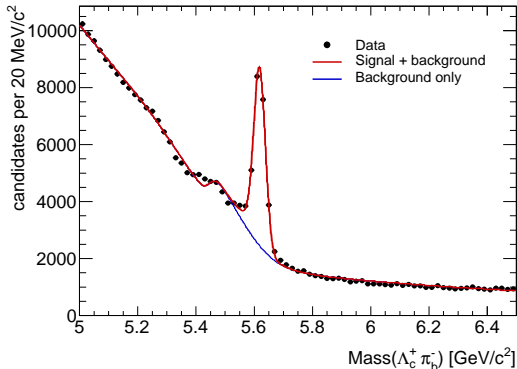


Figure 1: Invariant mass distribution of  $\Lambda_b^0 \rightarrow \Lambda_c^+ \pi_b^-$  candidates with a fit overlaid. The shoulder at the left sideband is dominated by fully reconstructed  $B$  mesons and partially reconstructed  $\Lambda_b^0$  decays.

approximately 2.6.

To reduce the background, a kinematic fit is applied to the resulting  $\Lambda_b^0$ ,  $\pi_s^-$  and  $\pi_s^+$  candidates that constrains them to originate from a common point. The  $\Lambda_b^0$  candidates are not constrained to the  $\Lambda_b^0$  mass in this fit. Furthermore, since the bottom-baryon resonance originates and decays at the primary vertex, the soft-pion tracks are required to originate from the primary vertex by requiring an impact parameter significance  $d_0(\pi_s^\pm)/\sigma_{d_0}$  smaller than 3 [11, 12], determined by maximizing the quantity  $S_{MC}/(1 + \sqrt{B})$ .

## 6 Results and Conclusions

The observed  $Q$ -value distribution is shown in Fig. 2. A narrow structure at  $Q \approx 21 \text{ MeV}/c^2$  is clearly seen. The projection of the corresponding unbinned likelihood fit is overlaid on the data. The fit function includes a signal and a smooth background. The signal is parametrized by two Gaussian functions with common mean, and widths and relative sizes set according to Monte-Carlo simulation studies. Approximately 70% of the signal function is a narrow core with  $0.9 \text{ MeV}/c^2$  width, while the wider tail portion has a width of about  $2.3 \text{ MeV}/c^2$ . The background is described by a second order polynomial. The fit parameters are the position of the signal and its event yield. The negative logarithm of the extended likelihood function is minimized over the unbinned set of  $Q$ -values observed. The fit over the  $Q$  range 6–75  $\text{MeV}/c^2$  finds  $17.3_{-4.6}^{+5.3}$  signal candidates at  $Q = 20.96 \pm 0.35 \text{ MeV}/c^2$ .

The significance of the signal is determined using a log-likelihood-ratio statistic,  $D = -2 \ln(\mathcal{L}_0/\mathcal{L}_1)$  [35, 36]. We define the hypothesis  $\mathcal{H}_1$  as corresponding to the

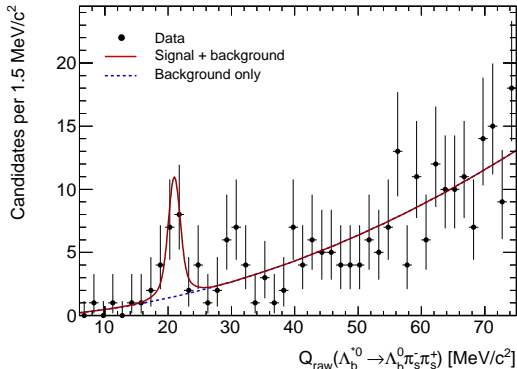


Figure 2: Distribution of  $Q$ -value for  $\Lambda_b^{*0}$  candidates, with fit projection overlaid.

presence of a  $\Lambda_b^{*0}$  signal in addition to the background and described by the likelihood  $\mathcal{L}_1$ . The null hypothesis,  $\mathcal{H}_0$ , assumes the presence of only background with a mass distribution described by the likelihood  $\mathcal{L}_0$ , and is nested in  $\mathcal{H}_1$ . The  $\mathcal{H}_1$  hypothesis involves two additional degrees of freedom with respect to  $\mathcal{H}_0$ , the signal position and its size. The significance for a  $Q$  search-window of 6–45  $\text{MeV}/c^2$  is determined by evaluating the distribution of the log-likelihood ratio in pseudoexperiments simulated under the  $\mathcal{H}_0$  hypothesis. The fraction of the generated trials yielding a value of  $D$  larger than that observed in experimental data determines the significance. The fraction is  $2.3 \times 10^{-4}$ , corresponding to a significance for the signal equivalent to 3.5 one-tailed Gaussian standard deviations.

The systematic uncertainties on the mass determination derive from the tracker momentum scale, the resolution model, and the choice of the background model. To calibrate the momentum scale, the energy loss in the tracker material and the intensity of the magnetic field must be determined. Both effects are calibrated and analyzed in detail using large samples of  $J/\psi$ ,  $\psi(2S)$ ,  $\Upsilon(1S)$ , and  $Z^0$  particles reconstructed in the  $\mu^+\mu^-$  decay modes as well as  $D^{*+} \rightarrow D^0(\rightarrow K^-\pi^+)\pi^+$ , and  $\psi(2S) \rightarrow J/\psi(\rightarrow \mu^+\mu^-)\pi^+\pi^-$  samples [37, 38]. The corresponding corrections are taken into account by the tracking algorithms. Any systematic uncertainties on these corrections are negligible in the  $Q$ -value measurements due to the mass difference term,  $m(\Lambda_b^0\pi_s^-\pi_s^+) - m(\Lambda_b^0)$ . The uncertainties on the measured mass differences due to the momentum scale of the low- $p_T$   $\pi_s^\pm$  tracks are estimated from a large calibration sample of  $D^{*+} \rightarrow D^0\pi_s^+$  decays. A scale factor of  $0.990 \pm 0.001$  for the soft pion transverse momentum is found to correct the difference between the  $Q$ -value observed in  $D^{*+}$  decays and its known value [3]. The same factor applied to the soft pions in a full simulation of  $\Lambda_b^{*0} \rightarrow \Lambda_b^0\pi_s^-\pi_s^+$  decays yields a  $Q$ -value change of  $-0.28 \text{ MeV}/c^2$ . Taking the full value of the change as the uncertainty, we adjust the  $Q$ -value determined by the fit to the

$\Lambda_b^{*0}$  candidates by  $-0.28 \pm 0.28$  MeV/ $c^2$ . The Monte-Carlo simulation underestimates the detector resolution, and the uncertainty of this mismatch is considered as another source of systematic uncertainty [12]. To evaluate the systematic uncertainty due to the resolution, we use a model with floating width parameter where only the ratio of the widths of the two Gaussians is fixed. The resulting uncertainty is found to be  $\pm 0.11$  MeV/ $c^2$ . To estimate the uncertainty associated with the choice of background shape, we increase the degree of the chosen polynomial and find the uncertainty to be  $\pm 0.03$  MeV/ $c^2$ . The statistical uncertainties on the resolution-model parameters due to the finite size of the simulated data sets introduce a negligible contribution. Adding in quadrature the uncertainties of all sources results in a total  $Q$ -value systematic uncertainty of  $\pm 0.30$  MeV/ $c^2$ .

Hence, the measured  $Q$ -value of the identified  $\Lambda_b^{*0}$  state is found to be  $20.68 \pm 0.35(\text{stat}) \pm 0.30(\text{syst})$  MeV/ $c^2$  [39]. Using the known values of the charged pion and  $\Lambda_b^0$  baryon masses [3], we obtain the absolute  $\Lambda_b^{*0}$  mass value to be  $5919.22 \pm 0.35(\text{stat}) \pm 0.30(\text{syst}) \pm 0.60(\Lambda_b^0)$  MeV/ $c^2$ , where the last uncertainty is the world's average  $\Lambda_b^0$  mass uncertainty reported in Ref. [3]. The result is closest to the calculation based on  $1/m_Q$ ,  $1/N_c$  expansions [9]. The result is also consistent with the higher state  $\Lambda_b^{*0}(5920)$  recently observed by the LHCb experiment [20]. LHCb also reports a state at approximately 5912 MeV/ $c^2$  [20]. Assuming similar relative production rates and relative efficiencies for reconstructing the  $\Lambda_b^{*0}(5912)$  and  $\Lambda_b^{*0}(5920)$  states in the CDF II and LHCb detectors, the lack of a visible  $\Lambda_b^{*0}(5912)$  signal in our data is statistically consistent within  $2\sigma$  with the  $\Lambda_b^{*0}(5912)$  yield reported by LHCb.

In conclusion, we conduct a search for the  $\Lambda_b^{*0} \rightarrow \Lambda_b^0 \pi^- \pi^+$  resonance state in its  $Q$ -value spectrum. A narrow structure is identified at  $5919.22 \pm 0.76$  MeV/ $c^2$  mass with a significance of  $3.5\sigma$ . This signal is attributed to the orbital excitation of the bottom baryon  $\Lambda_b^0$  and supports similar findings in proton-proton collisions.

## ACKNOWLEDGMENTS

I would like to thank the U.S. Department of Energy for supporting this work.

## References

- [1] M. Neubert, Phys. Rept. **245**, 259 (1994); A. V. Manohar and M. B. Wise, Camb. Monogr. Part. Phys. Nucl. Phys. Cosmol. **10**, 1 (2000).
- [2] N. Isgur and M. B. Wise, Phys. Lett. B **232**, 113 (1989); **237**, 527 (1990); Phys. Rev. D **42**, 2388 (1990).
- [3] J. Beringer *et al.* (Particle Data Group Collaboration), Phys. Rev. D **86**, 010001 (2012) and 2013 partial update for the 2014 edition.



- [4] J. G. Korner, M. Kramer, and D. Pirjol, *Prog. Part. Nucl. Phys.* **33**, 787 (1994).
- [5] Throughout the text the notation  $\Lambda_b^{*0}$  represents the  $J^P = \frac{1}{2}^-$  or the  $J^P = \frac{3}{2}^-$  state.
- [6] M. Karliner, B. Keren-Zur, H. J. Lipkin, and J. L. Rosner, *Annals Phys.* **324**, 2 (2009); M. Karliner, *Nucl. Phys. Proc. Suppl.* **187**, 21 (2009).
- [7] H. Garcilazo, J. Vijande, and A. Valcarce, *J. Phys. G* **34**, 961 (2007).
- [8] D. Ebert, R. N. Faustov, and V. O. Galkin, *Phys. Rev. D* **72**, 034026 (2005); *Phys. Lett. B* **659**, 612 (2008); *Phys. Atom. Nucl.* **72**, 178 (2009).
- [9] Z. Aziza Baccouche, C. -K. Chow, T. D. Cohen, and B. A. Gelman, *Phys. Lett. B* **514**, 346 (2001); *Nucl. Phys.* **A696**, 638 (2001).
- [10] J. R. Zhang and M. Q. Huang, *Phys. Rev. D* **78**, 094015 (2008); *Chin. Phys. C* **33**, 1385 (2009).
- [11] T. Aaltonen *et al.* (CDF Collaboration), *Phys. Rev. Lett.* **99**, 202001 (2007).
- [12] T. Aaltonen *et al.* (CDF Collaboration), *Phys. Rev. D* **85**, 092011 (2012).
- [13] V. M. Abazov *et al.* (D0 Collaboration), *Phys. Rev. Lett.* **99**, 052001 (2007).
- [14] T. Aaltonen *et al.* (CDF Collaboration), *Phys. Rev. Lett.* **99**, 052002 (2007).
- [15] T. Aaltonen *et al.* (CDF Collaboration), *Phys. Rev. D* **80**, 072003 (2009).
- [16] V. M. Abazov *et al.* (D0 Collaboration), *Phys. Rev. Lett.* **101**, 232002 (2008).
- [17] T. Aaltonen *et al.* (CDF Collaboration), *Phys. Rev. Lett.* **107**, 102001 (2011).
- [18] R. Aaij *et al.* (LHCb Collaboration), *Phys. Rev. Lett.* **110**, 182001 (2013)
- [19] S. Chatrchyan *et al.* (CMS Collaboration), *Phys. Rev. Lett.* **108**, 252002 (2012).
- [20] R. Aaij *et al.* (LHCb Collaboration), *Phys. Rev. Lett.* **109**, 172003 (2012).
- [21] D. Acosta *et al.* (CDF Collaboration), *Phys. Rev. D* **71**, 032001 (2005).
- [22] T. Aaltonen *et al.* (CDF Collaboration), *Nucl. Instrum. Methods A* **729**, 153 (2013).
- [23] A. A. Affolder *et al.*, *Nucl. Instrum. Methods A* **526**, 249 (2004).

- [24] We use a cylindrical coordinate system with  $z$  axis along the nominal proton beam line, radius  $r$  measured from the beam line and  $\phi$  defined as an azimuthal angle. The transverse plane  $(r, \phi)$  is perpendicular to the  $z$  axis. The polar angle  $\theta$  is measured from the  $z$  axis. Transverse momentum  $p_T$  is the component of the particle's momentum projected onto the transverse plane. Pseudorapidity is defined as  $\eta \equiv -\ln(\tan(\theta/2))$ . The impact parameter of a charged particle track  $d_0$  is defined as the distance of closest approach of the particle track to the point of origin (primary vertex) in the transverse plane.
- [25] E. J. Thomson *et al.*, IEEE Trans. Nucl. Sci. **49**, 1063 (2002).
- [26] B. Ashmanskas *et al.*, Nucl. Instrum. Methods A **518**, 532 (2004); L. Ristori and G. Punzi, Ann. Rev. Nucl. Part. Sci. **60**, 595 (2010).
- [27] P. Nason, S. Dawson, and R. K. Ellis, Nucl. Phys. **B303**, 607 (1988); **B327**, 49 (1989).
- [28] C. Peterson, D. Schlatter, I. Schmitt, and P. M. Zerwas, Phys. Rev. D **27**, 105 (1983).
- [29] D. J. Lange, Nucl. Instrum. Methods A **462**, 152 (2001).
- [30] R. Brun, R. Hagelberg, M. Hansroul, and J.C. Lassalle, CERN Reports No. CERN-DD-78-2-REV and No. CERN-DD-78-2.
- [31] All references to a specific charge combination imply the charge conjugate combination as well.
- [32] G. Punzi, in *Proceedings of the Conference on Statistical problems in particle physics, astrophysics and cosmology, PHYSTAT 2003, Stanford, USA, September 8-11, 2003*, edited by L. Lyons, R. P. Mount and R. Reitmeyer (SLAC, Stanford, 2003), p. 79. eConf C **030908**, MODT002 (2003). [arXiv:physics/0308063]
- [33] A. Abulencia *et al.* (CDF Collaboration), Phys. Rev. Lett. **98**, 122002 (2007).
- [34] T. Aaltonen *et al.* (CDF Collaboration), Phys. Rev. Lett. **104**, 102002 (2010).
- [35] S. S. Wilks, Ann. Math. Statist. **9**, 60 (1938).
- [36] R. Royall, J. Amer. Statist. Assoc. **95**, 760 (2000).
- [37] D. Acosta *et al.* (CDF Collaboration), Phys. Rev. Lett. **96**, 202001 (2006).
- [38] T. Aaltonen *et al.* (CDF Collaboration), Phys. Rev. Lett. **103**, 152001 (2009).
- [39] T. A. Aaltonen *et al.* [CDF Collaboration], Submitted to: Phys.Rev.D (RC) [arXiv:1308.1760 [hep-ex]].